European Journal of Pharmaceutical Sciences 158 (2021) 105690

Contents lists available at ScienceDirect

European Journal of Pharmaceutical Sciences

journal homepage: www.elsevier.com/locate/ejps

Preparation and Characterization of Protein-loaded PFC Nanoemulsions for the Treatment of Heart Diseases by Pulmonary Administration

Xichun Qin [a,#], Yeqing Zhou [a,#], Yuzhuo Wang [a], Ziyao Wang [c], Yun Wang [c], Jiali Chen [a], Lidong Zhu [a], Xiaoyu Quan [a], Zhiwei Liu [b], Hao Zhang [a], Liqun Jiang [c,*], Hongyan Dong [b,*], Zhongming Zhang [a,*]

[a] Department of Thoracic Cardiovascular Surgery, Affiliated Hospital of Xuzhou Medical University, China
[b] Morphological Research Experiment Center, Xuzhou Medical University, China
[c] Jiangsu Key laboratory of New Drug research and clinical Pharmacy, Xuzhou Medical University, China

ARTICLE INFO

Keywords:
Inhalation
Protein-phospholipid complexes
PFC
Nanoemulsion
Heart target
Drug delivery

ABSTRACT

In the treatment of heart disease, strategies for the targeted delivery of protein therapeutics to the heart by inhalation are still immature. Perfluorocarbons (PFCs) are inert chemicals with good biocompatibility, and unique physico-chemical properties that have recently led to their applications in numerous fields. In this study, we combined the advantages of protein-phospholipid complexes and PFC emulsions and then synthesized protein-loaded PFC nanoemulsions (PNEs) to test whether, after inhalation, these nanoemulsions could deliver therapeutic proteins to the heart. After preparing protein-phospholipid complexes by lyophilization, we obtained PNEs by extrusion. The particle size and surface charge of PNEs were about 140 nm and -50 mV, respectively. *In vitro* results showed that the PNEs had a fine particle fraction of 35% and exhibited sustained protein release. Translocation studies were done using three types of pulmonary epithelial cells, and ~7% translocation was observed in the Calu-3 cell line. Further, they were easily absorbed by cells and had therapeutic effects in culture. *In vivo* results showed that the PNEs successfully delivered proteins to the myocardial tissue of rats and reduced ischemic myocardial injury caused by acute myocardial infarction (AMI). This study suggests that inhalation of PNEs is a new potential strategy to deliver proteins to cardiac tissues for treating heart diseases.

1. Introduction

With the advent of proteomics, the development of therapeutics based on proteins/peptide drugs (hereafter called proteins) has attracted significant academic and commercial attention (Bull and Doig, 2015). Through the research and development of macromolecular drugs, the potential clinical value of protein drugs has become increasingly evident (Lagasse et al., 2017). Cardiovascular diseases are the leading contributors to disease burden in older people (30.3% of the total burden in people aged 60 years and older) (Prince et al., 2015). However, in the treatment of heart disease, the targeted delivery of drugs, especially protein drugs, requires further study (Liu et al., 2014).

On the basis of anatomy, after inhaled drugs such as nanomaterials are absorbed, they can cross respiratory barrier to reach systemic circulation and secondary organs. (Puisney et al., 2018) (Miragoli et al., 2018). The ideal carrier is necessary for pulmonary administration (Asmawi et al., 2019) (Arbain et al., 2019). Aerosols have their limitations, it is difficult to deliver drugs deep into the lungs or in places filled with fluid (Jaafar-Maalej et al., 2009). Nanoparticles can cross the alveolar-capillary barrier, demonstrating that inhalation therapy could be used for the treatment of heart disease (Miragoli et al., 2018) (Braakhuis et al., 2015). However, there are also some disadvantages to the use of nanoparticles. For example, strong interactions between individual nanoparticles can lead to agglomeration (Naahidi et al., 2013). Further, there is a risk that they might deposit deep in the lungs and might cause damage (Braakhuis et al., 2014).

Perfluorocarbons (PFCs) are a promising carrier for pulmonary administration. PFCs are not metabolized in the body and can be

* Corresponding authors at: Department of Thoracic Cardiovascular Surgery, Affiliated Hospital of Xuzhou Medical University, 99 West Huaihai Road, Xuzhou 221006, Jiangsu, China.
E-mail addresses: 100002014025@xzhmu.edu.cn (L. Jiang), dhy@xzhmu.edu.cn (H. Dong), zhang_zhongming@xzhmu.edu.cn (Z. Zhang).
# These authors contributed equally.

https://doi.org/10.1016/j.ejps.2020.105690
Received 13 July 2020; Received in revised form 30 November 2020; Accepted 20 December 2020
Available online 24 December 2020

excreted by breathing (Li et al., 2018). PFC's low surface tension, high density, and high diffusion coefficient allows PFC-based particles to flow through extremely narrow airways (Lehmler, 2007). More importantly, oxygen is dissolved in PFCs at a concentration of about 40%–50%, which is 20 times higher than the capacity of water and 2 times higher than plasma (Lowe, 1999). We speculate that these properties allow PFCs to enhance blood gas exchange and enable drug delivery. Pigment epithelium-derived factor (PEDF) is a highly conserved secreted pleiotropic monomeric glycoprotein naturally present in the body (Tombran-Tink and Barnstable, 2003). It has been shown to play a central role in mediating cellular protection against oxidative stress, by promoting cell survival, reducing inflammation, and inhibiting pathological angiogenesis in a range of cell types and tissues (Brook et al., 2020). PEDF is thought to exert its biological activity by interacting with its receptor on cell surface (Yuan et al., 2019). Our previous studies have shown that PEDF has protective effects on the myocardium during acute myocardial infarction (AMI) in rats (Yuan et al., 2019) (Qiu et al., 2018). However, the cardiac delivery of PEDF as well as the suitable drug carrier are in great need to induce this effect.

To date, PFCs have rarely been reported as carriers for protein drugs (Li et al., 2018). Because PFCs are immiscible with water, they are often applied in the form of emulsions. PFC emulsions are classified into oil-in-water (O/W) type and water-in-oil (W/O) type, and proteins are usually hydrophilic and thus present in the aqueous phase. For O/W emulsions, the proteins will quickly diffuse into the external aqueous environment, leading to burst release and only a small remaining amount of protein drug by the time the carrier gets to the target. For W/O emulsions, phase inversion may happen *in vivo*, also leading to drug loss (Rao and Shao, 2008). Some studies have shown that protein-phospholipid complexes can enhance the lipophilicity of proteins (Zhang et al., 2012). Considering that O/W nanoemulsions are easily atomized and have higher patient compliance, enhancing the lipophilicity of the protein and loading it into the oil phase of the O/W nanoemulsion is highly desirable.

The purpose of this study was to develop a new type of protein-loaded PFC nanoemulsion (PNE), with a goal of testing whether PFC nanoemulsions can cross the alveolar-capillary barrier and deliver proteins to cardiac tissues for the treatment of heart diseases.

2. Materials and Methods

2.1. Materials

Hydrogenated Soybean Phospholipids (HSPC) were purchased from Ai Weituo (Shanghai) Pharmaceutical Technology Co., Ltd. (Shanghai, China). Bovine Serum Albumin (BSA) was purchased from Shanghai Huixing Biochemical Reagent Co., Ltd. (Shanghai, China). Recombinant rat PEDF (GenBank accession number: NM_177927) was synthesized by Cusabio Biotech, Co, Ltd (Wuhan, China). Perflubron (PFOB) was purchased from Shanghai Aladdin Biochemical Technology Co., Ltd. (Shanghai, China). All the other reagents were of analytical grade.

2.2. Preparation and Characterization of PNEs

2.2.1. Preparation and Oil-water Partition Determination of Protein-phospholipid Complex

The protein-phospholipid complexes was prepared with proteins (BSA, bovine serum albumin, molecular weight: 66 kDa, molecular diameter: 14 nm (Tencer et al., 2007); PEDF, pigment epithelium-derived factor, molecular weight: 50 kDa, molecular diameter: 7 nm (Becerra, 2006)) and HSPC at various weight ratios (1:0, 1:1, 1:5, 1:10, 1:15, 1:20). HSPC was dissolved in absolute ethanol (100 mg/ml), and proteins were dissolved in sodium dihydrogen phosphate (NaH_2PO_4) buffer at pH = 6.5 (1 mg / ml) to enhance charge transfer effect (The isoelectric point of PEDF is 6.0 and that of BSA is 4.7. The isoelectric point of phospholipid used in this study (HSPC) is 7.0. When pH of the buffer was set at 6.5, the proteins possessed negative charges and phospholipid possessed positive charges, inducing the charge effect to form the protein-phospholipid complex) (Khan et al., 2013). After mixing, solutions were stirred for 2 h and put it in a refrigerator at -20°C overnight. The protein-phospholipid complexes was freezed at -40°C for 12h, and then lyophilized (FD-1C-50, Beijing Boyikang Experimental Instrument Co., Ltd., Beijing, China). The cold trap of the freeze dryer was -45°C and the degree of vacuum was 10 mPa.

Three milligrams of protein-phospholipid complexes were dissolved in 3 ml of a mixture of water and PFOB (4: 1, v / v), mixed thoroughly, centrifuged at 14,000 g for 15 min. Then, 1 ml of supernatant was placed into a vial along with 4 ml Coomassie brilliant blue G250 solution, and distilled water was added to a total volume of 10 ml. This solution was kept at room temperature for 35 min. Samples containing no protein or containing the same concentration of protein were processed identically as a reference, and absorbance was measured at 595 nm. The oil-water distribution coefficient was calculated based on absorbance.

2.2.2. Preparation of PNEs

The composition of PNE (1ml) consists of three parts: (1) Oil phase: 80 μl PFOB; (2) Emulsifier: 40 mg protein-phospholipid complexes, 20 mg HSPC, 30 mg PEG-4000, 20 mg Vitamin E-TPGS; (3) Water phase: 920 μl deionized water. After magnetic stirring, the preparation was extruded 15 times through a 0.1 μm filter in the MiniExtruder system (Avanti Polar Lipids, AL, USA). Finally, it was filtered through a sterile filter (0.1 μm) and stored at 8°C.

2.2.3. Particle Size and Zeta Potential Determination

The particle size and surface charge of PNEs were determined by dynamic light scattering using the PSS NICOMP 380 ZLS Zeta potential/particle sizer (Preferred Systems Solutions, Inc., Santa Barbara, CA, USA). To prove the correction of the results, the samples were diluted with PBS (pH 7.2) to control the average count rates of the sample in the range of 100-300. The parameters of the detection were set as followings: channel width: 6.4 uSec; temperature: 23°C; liquid viscosity: 0.933 CP; liquid index of refraction: 1.333; intensity setpoint: 300 KHz; external fiber angle: 90 deg; scattering angle: 90 deg; numbers of measuring cycles: 3.

2.2.4. Morphology Determination

The morphology of PNEs was examined by transmission electron microscopy (TEM, Tecnai G2 Spirit Twin; FEI Company, Hillsboro, OR, USA). Briefly, PNEs were diluted 100 × with distilled water, and a drop of the suspension was deposited on a copper mesh coated with a formvar film. After removing excess fluid, the sample was negatively stained with 2% phosphotungstic acid for about 30 seconds, and then the sample was examined with TEM.

2.2.5. Protein Release Determination in Vitro

The protein release from 0.5 ml of PNEs was detected in 4.5 mL PBS (pH 7.4) or bronchoalveolar lavage fluid (BALF) at 37°C (BALF, see section 2.8). At different time points (0 h, 1 h, 2 h, 4 h, 8 h, 12 h, 24 h), 100 μl of sample was aspirated, centrifuged at 14,000 g for 15 min, and then the supernatant was collected to measure protein concentration. The protein concentration in each sample was determined using the bicinchoninic acid (BCA) method according to the manufacturer's instructions. (Biyuntian BCA protein quantification kit, # P0012). In this study, the protein release within only 24h was performed, because the nanoemulsion stays in the lungs of rats for no more than 24h, which was proved in Section 3.8.

2.2.6. Fine Particle Fraction Determination

The fine particle fraction determination of PNEs released from these devices was evaluated using a twin impinger (British Pharmacopoeia 2010, Appendix XII C7, Apparatus A). Cou-6-PNEs (6 mL, 10 × diluted, see section 2.4) were placed in a tube that was connected to a nebulizer

(NE-C900, OMRON, Japan). A flow rate of 60 L/min was obtained using a vacuum pump. The upper and lower stages of the impinger were filled with 7 mL and 25 mL of a 1:1 (v / v) mixture of methanol-water. After the atomization process was over, the samples were taken from the lower and upper stages for analysis of drug content using fluorescence spectrophotometry (F-4600, Hitachi Ltd., Tokyo, Japan). The fraction that was deposited in the lower stage of the impinger represented the fine particle fraction (FPF) of PNEs.

2.3. Cell Culture and Cytotoxicity of PNEs

The embryonic rat heart-derived H9c2 cell line was obtained from the American Type Culture Collection. RLE-6TN rat lung epithelial type II cells was obtained from the Wuhan Procell Life Technology Co., Ltd. Human non-small cell lung cancer A549 cell line and human lung adenocarcinoma Calu-3 cell line were gifts from Cancer Institute of Xuzhou Medical University. All cells were cultured in DMEM high glucose medium containing 10% fetal bovine serum and were incubated in a humidified atmosphere containing 5% CO_2. We replaced the medium every 2 days. The digestion process used a solution of trypsin / EDTA (0.25% trypsin). Hypoxia was achieved by culturing cells in DHank's liquid with glucose deprivation in a tri-gas incubator saturated with 5% CO_2 / 1% O_2 at 37°C for the indicated time periods (Heal Force, Shanghai, China). All cells were sub-cultured or used for experimental procedures at 80-90% confluence.

Cells (1×10^4 cells per well) were seeded into wells of a 96-well plate (Corning, New York, USA). Cell viability was assessed using a CCK-8 kit (Dojindo Molecular Technologies, Inc., Tokyo, Japan). The absorbance at 450 nm was measured using a microplate reader (BioTek Synergy2, Instruments, Inc., Winooski, VT, USA). The mean optical density (OD) value from at least 3 parallel groups was used to calculate the cell viability.

2.4. Transport of PNEs

Proteins (BSA and PEDF) were dissolved in a sodium dihydrogen phosphate (NaH2PO4) buffer solution with a pH of 6.5 (1 mg/ml), and Cy5-NHS solution (1 mg/ml, DMSO) was slowly added under magnetic stirring. The weight ratio of proteins and Cy5-NHS was 200: 1. The NHS (N-HydroxySuccinimide) group could react with the amino group of proteins to induce stable chemical bindings of Cy5 with proteins (Jiang et al., 2019). After the reaction performed at 25°C for 12 hours, the mixed sample was placed in a dialysis bag (MW: 14,000 Da), and then the dialysis bag was placed in 1 L of acetic acid aqueous solution (PH 6.0) for 2 days with stirring, and the acetic acid solution was replaced every 12 h. After dialysis, the sample was lyophilized to obtain Cy5-proteins. The lyophilization procedure was the same as mentioned in Section 2.2.1. About 43.7% fluorescence intensity was retained after dialysis and lyophilization compared to input. The Cy5-proteins were prepared formulated into Cy5-B-PNE or Cy5-P-PNE as described above, with protein replaced by Cy5-protein. Coumarin is lipophilic and can be used to represent the oil phase. A small amount of coumarin 6 (Sigma-Aldrich) was dissolved in PFOB (10 μg/ml), and Cou-6-PNEs were obtained using the method of preparing PNEs.

To detect the transport of PNEs, three alveolar epithelial cells stabilized (A549, RLE-6TN and Calu-3) were seeded on the upper chamber of a transwell (1×10^5 per well, 0.4 μm pore polyester membrane, Corning, New York, USA) and cultured for 10 days. Incubating cell monolayers with B-PNE for 12h, after refreshing the culture medium, transepithelial electrical resistance (TEER) was measured by EVOM2 (WPI, Sarasota, USA). The mean resistance of a cell-free transwell insert was subtracted from the resistance measured across each cell layer to yield the TEER value of the cell monolayer. The mean transport rate of PNEs was measured by fluorescence spectrophotometry. Cou-6-B-PNE (BSA, 10 μg / ml) were added to phenol red-free medium in the upper chamber and incubated for 1, 2, 4, 8, 12 h, than collected medium in the lower chamber of transwell for the next experiment. Coumarin 6 was insoluble in water, if coumarin 6 was detected in the lower chamber of transwell, it meant that PNEs could cross the cell monolayer.

2.5. Intracellular Uptake

To track the intracellular localization, after incubation of cells with Cou-6-B-PNE for 12 h, the cells were labeled with a Lyso Tracker Red DND-99 and fixed with paraformaldehyde. The location of PNEs in the cells was observed using a laser confocal scanning microscopy (Olympus FV10i, Tokyo, Japan).

H9c2 cells (1×10^4 per well) were seeded into wells of a 96-well plate (Corning, New York, USA), and then Cou-6-B-PNE (BSA, 10 μg / ml) were added and incubated for 1, 2, 4, 8, 12 h. Nuclei were counterstained with 4,6-diamidino-2-phenylindole (DAPI; KeyGen Biotech, catalog #KGA215–10, China). After 3 washes in PBS, samples were directly observed using a fluorescent microscope (Olympus, Tokyo, Japan). Intracellular Cou-6 was detected using a multimode microplate reader (Synergy2; BioTek,Winooski, VT, USA) at 366 nm.

2.6. Western Blotting Analysis

To prepare a whole cell lysate, cells were lysed with a Cell Total Protein Extraction Kit (catalog #C510003, Sangon Biotech) containing a cocktail of phosphatase inhibitors and protease inhibitors. Rat tissue proteins in the myocardium of the infarct zone were extracted with lysis buffer (pH=7.5) containing 50 mM Tris, 150 mM NaCl, 0.1% SDS, 1% Triton X-100, 1% Na-deoxycholate, 1% protease, and complete protease inhibitor cocktail (catalog #C510003, Sangon Biotech).

Primary antibodies against cleaved caspase-3 (1:1,000, catalog # 9661, CST), PEDF (1:1,000, catalog # DF6547, Affinity Biosciences) and β-tubulin (1:20,000, catalog # 66240-1-Ig, Proteintech) were used, followed by corresponding secondary antibodies (anti-rabbit IgG H+L DyLight™800 4 × PEG 1:30,000; cat. no. 5151, and anti-mouse IgG H+L DyLight™ 680 1:15,000; cat. no. 5470, Cell Signaling Technology), and images were captured using the Odyssey infrared imaging system (LI-COR Biosciences, Lincoln, NE, USA). Western blot results were quantified using ImageJ software (National Institutes of Health, Bethesda, MD). Relative protein expression was calculated after normalization to β-tubulin.

2.7. Effect of PNEs on AMI in Rats

2.7.1. Rats

Sprague-Dawley (SD) male rats (250 ± 20 g, 8-10 weeks) were obtained from the Experimental Animal Center of Xuzhou Medical College. The rats were kept on a 12 h light-dark cycle with free access to food and water. All experiments were performed in adherence with the National Institutes of Health (NIH Publication, 8th Edition, 2011) guidelines for the use of laboratory animals. The rat care and experimental protocols were approved by the Animal Care and Use Committee of Xuzhou Medical University (License no. SYXK 2002-0038; Jiangsu, China).

SD rats were anesthetized with sodium pentobarbital (60 mg / kg) intraperitoneally. After adequate anesthesia, PNEs were administered by oral tracheal intubation. In addition, using a 16-gauge polyethylene catheter connected to a ventilator (Medical Equipment Company, Shanghai, China) for artificial respiration three minutes to prevent asphyxia. One dose of PNE (protein, 2 mg / kg) or an equal volume of normal saline was administered via the catheter.

The AMI model was induced by ligation of the left anterior descending (LAD) coronary artery (Qiu et al., 2018). In brief, placing rats in a supine position, a left thoracotomy was performed through the fourth intercostal space under sterile conditions. Following thoracotomy, a 6-0 Prolene® monofilament polypropylene suture (Ethicon, Somerville, NJ) was passed from below to loop the LAD and then tightened. After successful ligation, the left ventricular myocardium

changed from bright red to dark purple and the ECG showed ST-segment elevation.

2.7.2. Histological Examination

After the rats were sacrificed, the heart and left lung was fixed in 4% paraformaldehyde, dehydrated, embedded in paraffin, and then the tissue was cut into 4 μm sections and stained with hematoxylin-eosin to assess pathology.

Frozen sections of myocardium and lung (8 μm) were fixed for 15 minutes with 4% paraformaldehyde, nuclei were stained with 40, 6-diamidino-2-phenylindole (catalog # KGA215–10; KeyGEN BioTECH Corp., Ltd,Nanjing, China). After a final wash, coverslips were mounted on slides using 50% glycerin. Then, sections were observed using a confocal laser scanning microscope.

2.7.3. Determination of Myocardial Infarct Size and Glycogen Content Assay

Hearts were frozen at -20 °C and cut into 2 mm slices perpendicular to the axis of the left anterior descending coronary artery. Slices were immediately immersed in 1% TTC (Sigma-Aldrich) in phosphate buffer (pH 7.2) at 37°C for 15 minutes to discriminate infarcted tissue from viable myocardium (Li et al., 2018). All slices were scanned by a color CCD camera (FV-10; Fujifilm, Tokyo, Japan). Morphometric measurements of the infarct area (INF) were performed with digital planimetry software (Image-Pro Plus 6.0; Media Cybernetics Inc., Bethesda, MD). The myocardial infarct size was expressed as a percentage of the infarct area (INF) over total LV (INF/ LV × 100%).

Periodic Acid Schiff (PAS) Glycogen Staining was performed using a Periodic Acid-Schiff (PAS) Kit (395B, Sigma-Aldrich). Semithin sections or Cardiomyocytes were fixed with 4% paraformaldehyde, oxidized with periodic acid for 5 minutes at room temperature, washed, and then incubated in Schiff's reagent for 15 min at room temperature. Then, they were washed and counterstained with hematoxylin solution for 90 seconds, washed, dehydrated, and, last, the cover slips were mounted on slides using 50% glycerin. Images were acquired using a color CCD camera (FV-10, Fujifilm). Glycogen contents were measured using a two enzymes, colorimetric glucose assay by Glycogen Assay Kit following the manufacturer's instructions (MAK016, Sigma-Aldrich). Relative quantitative analysis of the change in glycogen levels was normalized to the normal group.

2.8. Bronchoalveolar Lavage

After the rats were sacrificed, the chest cavity was opened with a midline incision. Bronchoalveolar lavage was performed from the lung through a tracheal cannula with 5 ml cold PBS (pH 7.2). This procedure was repeated three times. After centrifugation at 4°C and 1000 g for 10 min, the cell-free supernatant was collected. Levels of TNF-α, IL-1β and IL-6 were measured using quantitative enzyme-linked immunosorbent assay analysis (ELISA) kits according to the manufacturer's protocols (Shanghai Renjie Biotechnology Co., Ltd, Shanghai, China).

2.9. Effect of PNEs on Blood Gas Analysis

Blood gas was measured at the exposed femoral arteries while rats were under deep anesthesia. After rats were treated with an inhaled dose of B-PNE or an equal volume of normal saline, samples (0.5 mL) of blood were taken from abdominal aorta using an Arterial Blood Gas Sampler (3302, 3cc; Westmed,Inc, Tucson, AZ). Samples were analyzed by an automated blood gas system (GEM Premier 3500; Instrumentation Laboratory, Bedford, MA).

2.10. Statistical Analysis

Data were expressed as means ± standard deviation (SD). Multiple group comparisons were evaluated via one-way analysis of variance (ANOVA) followed by least significant difference -t-test for post hoc analysis. Data between 2 independent groups were compared using two-tailed Student's t- test. Analyses were performed using SPSS software (Chicago, IL, USA). $P<0.05$ was considered to represent a significant difference.

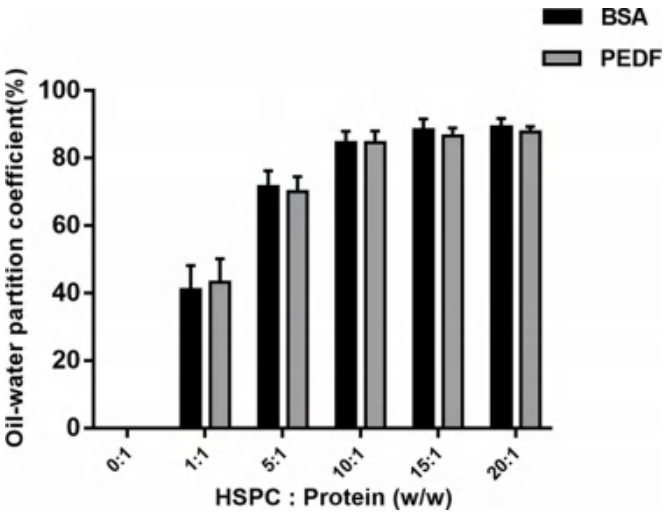

Fig. 1. Oil-water partition coefficient of protein-phospholipid complexes. Data are expressed as mean ± SD (n = 3).

Results

3.1. Characterization of Protein-phospholipid Complexes

Before preparing PNEs, protein-phospholipid complexes were first prepared. After binding to phospholipids, the protein will be more lipophilic (Zhou et al., 2012). First of all, in this experiment, BSA, was selected for synthesis of the BSA-phospholipid complex. Secondly, we synthesized PEDF-phospholipid complex. PEDF has previously been proved to have clear protective effects on the myocardium during acute ischemia (Yuan et al., 2019) (Yuan et al., 2019). The oil-water partition coefficient was measured to determine the lipophilicity of the complex. We found that, when the weight ratio of phospholipid to protein reached more than 10:1, the lipophilicity of both proteins was significantly improved, and the oil-water partition coefficients were around 85% (Fig. 1). On the basis of this finding, we used a weight ratio of phospholipid to protein of 15:1 in the following experiments.

3.2. Characterization of PNEs

In order to avoid damage to the protein structure and protein-phospholipid complex caused by high-pressure homogenization or phacoemulsification, control nanoemulsions loaded with BSA were prepared using a MiniExtruder (filter size 0.1 μm). The resulting emulsion was named BSA-phospholipid complex perfluorocarbon nanoemulsion (B-PNE). The therapeutic nanoemulsion loaded with the protein PEDF was called PEDF-phospholipid complex perfluorocarbon nano-emulsion (P-PNE). In addition to the surfactant, the components of the emulsifier included phospholipids and protein-phospholipid complexes, and the theoretical maximum drug loading was 3.75 mg / ml. In this experiment, the drug loading we actually achieved was 2.5 mg / ml.

Smaller droplet sizes allow for a greater degree of drug absorption and utilization (Liu et al., 2009). The size and stability of the emulsion drops were evaluated by observing their morphological characteristics and zeta potentials. The respective emulsion particle sizes were 138.9 ± 3.7 nm and 140.1 ± 4.7 nm (Fig. 2A), and the Zeta potentials were -50.27 ± 1.26 mV, -50.13 ± 1.83 mV (Fig. 2B). We also investigated the protein-unloaded perfluorocarbon nanoemulsion (U-PNE). The

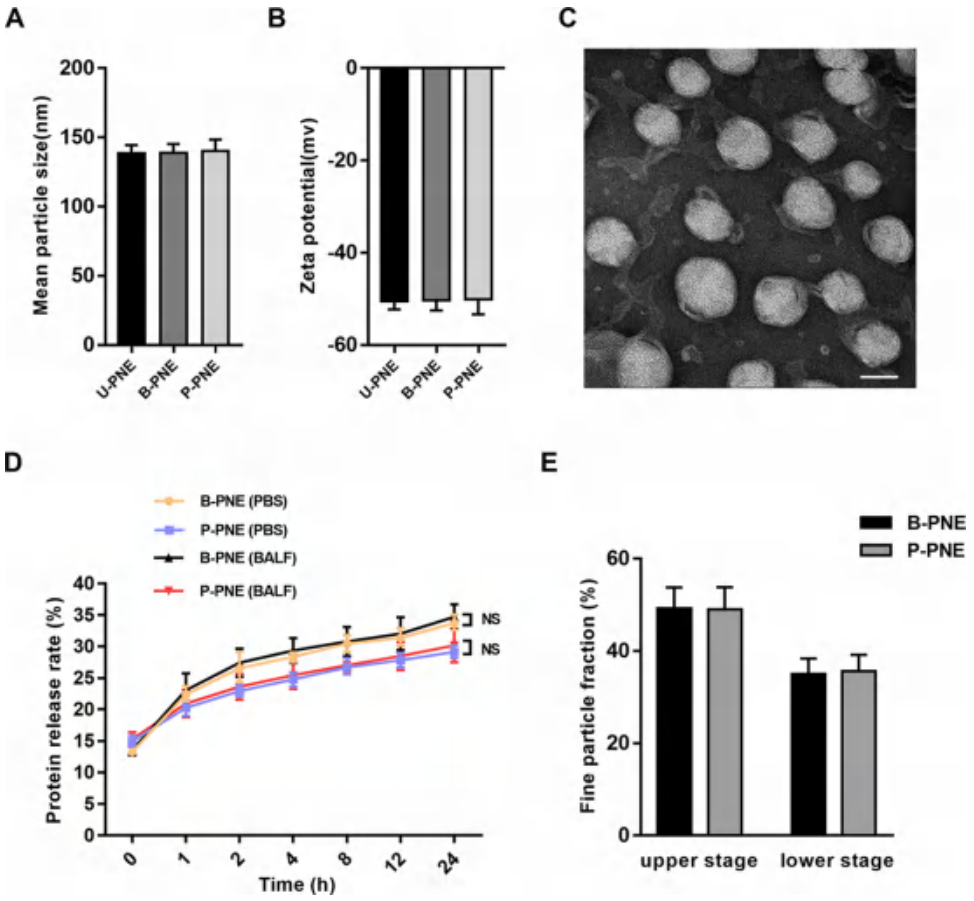

Fig. 2. Characterization of PNEs. (A) The mean particle size of PNEs. (B) The zeta potential of PNEs. U-PNE, protein-unloaded perfluorocarbon nanoemulsion; B-PNE, BSA-phospholipid complex perfluorocarbon nanoemulsion; P-PNE, PEDF-phospholipid complex perfluorocarbon nano-emulsion. (C) Representative transmission electron micrograph of PNEs (the typical characteristics of P-PNE), bar = 100 nm. (D) The protein release rate of PNEs. (E) The fine particle fraction of PNEs. Data are expressed as mean ± SD (n = 3).

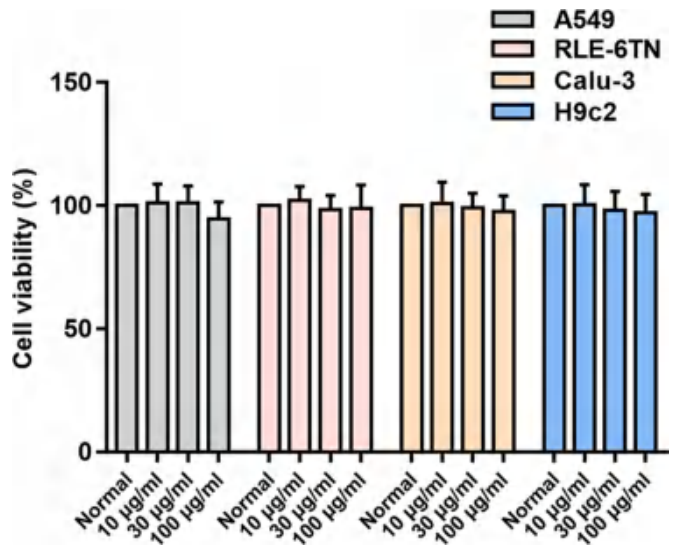

Fig. 3. Cytotoxicity of PNEs. B-PNE treatment of A549, RLE-6TN, Calu-3, H9c2 cells with BSA concentrations of 10 μg / ml, 30 μg / ml, and 100 μg / ml respectively by CCK-8 assay after 48 hours of incubation. Data are expressed as mean ± SD (n = 3).

physicochemical characteristics of U-PNE, B-PNE and P-PNE were relatively consistent (Fig 2A-B). TEM imaging showed that the emulsion droplets were uniformly sphere (Fig. 2C).

3.3. Protein Release Rate of PNEs

The release characteristics of PNEs *in vitro* was determined as shown in Fig. 3A. The release rate of BSA in B-PNE increased from 13.2 ± 0.3% at 0 h to 32.7 ± 1.0% after 24 h, and the release rate of PEDF from P-PNE increased from 15.0 ± 0.5% at 0 h to 29.1 ± 0.7% after 24 h (Fig. 2D). This suggested that the lipophilicity of the protein was improved after binding to phospholipids, yielding a sustained rate of release. In addition, there was no significant difference in the protein release rate of PNEs in BALF and PBS, which indicated that alveolar surfactant might not affect the protein release of PNEs. It was noteworthy that the protein release rate and oil-water partition coefficient at 0 h between the two formulations were essentially the same.

3.4. Fine Particle Fraction of PNEs

Inhalation formulations require assessment of the fraction of fine particles. Therefore, we used coumarin 6 to label the oil phase of PNEs and then measured the pulmonary sedimentation coefficient to predict whether the nanoemulsion could be used for pulmonary administration after ultrasonic atomization. The fraction of coumarin 6-labeled PNEs that were deposited in the lower stage of the impinger was detected, suggesting that the fine particle fraction of PNEs was 35% (Fig. 2E), suggesting that 35% of PNEs would be predicted to settle in the lower respiratory tract after inhalation. These results indicated that the PNEs could be suitably prepared for pulmonary administration via ultrasonic atomization.

3.5. Cytotoxicity of PNEs

Although the safety of PFC emulsions and phospholipids have been

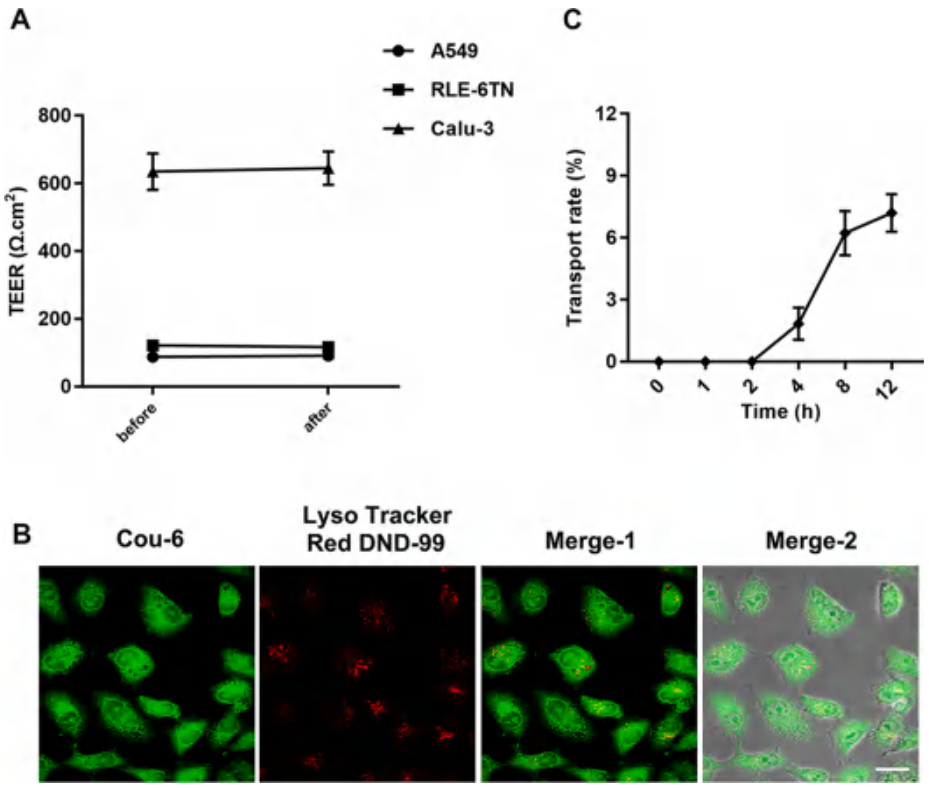

Fig. 4. Translocation and location of PNEs. (A) Influence of B-PNE on TEER of alveolar epithelial cells (after incubation compared to before incubation, n=3). (B) The location of Cou-6-B-PNE in the Calu-3 and H9c2 cells, which were labeled with lyso Tracker red (n=3). (C) Translocation of Cou-6-B-PNE through a Calu-3 monolayer. 60 × Objective lens; bar = 10 μm.

supported by numerous prior studies (Gonzalez-Rothi et al., 1991, Courrier et al., 2003, Shi et al., 2009), the incorporation of multiple surfactants may present new risks. Therefore, we used CCK-8, a sensitive colorimetric viability assay, to evaluate the toxicity of B-PNE to cells at different concentrations (PEDF may affect the characteristics of cells, so in some experiments we did not choose P-PNE). After treatment for 48 hours, across a 10 μg / ml to 100 μg / ml range of concentrations of BSA-loaded nanoemulsions, PNEs had no obvious toxic effect on alveolar epithelial cells and H9c2 cells (Fig. 3, $P > 0.05$), indicating that the PNEs were highly safe and could likely be used *in vivo*.

3.6. Translocation Study on Alveolar Epithelial Cell Monolayer

To study translocation of PNEs, B-PNE were added to the upper chamber of transwell. After 12 h of incubation of the alveolar epithelial cells (A549, RLE-6TN and Calu-3) monolayer with B-PNE, all TEER values were not significantly changed (Fig. 4A). We noticed that the TEER values of the A549 and RLE-6TN were too low, so we choosed the Calu-3 cell line for further study.

The protein-phospholipid complexes were attached to the surface of PFOB to form the oil phase. Considering that part of proteins were present in the aqueous phase of PNEs, Coumarin 6 was insoluble in water, so it could represent the oil phase. We tracked the localization of PNEs firstly, after incubating the Calu-3 cells with Cou-6-B-PNE for 12h, Calu-3 cells were labeled with Lyso Tracker Red DND-99, which was typically used to specifcally label lysosomes. Laser confocal microscopy showed that the green fluorescence was evenly distributed in the cytoplasm, no obvious overlap with the red fluorescent regions (Fig. 4B). This result indicated that the PNEs taken up by the cells were not targeted to lysosomes.

The translocation of Cou-6-B-PNE is shown in Fig. 4C. After incubating the Calu-3 cells with Cou-6-B-PNE on the 0.4 μm pore size membrane, we could not detect any translocation within 2h, but as time prolonged, Coumarin 6 kept accumulating in the lower chamber (7.2 ± 0.5% translocation was observed at 12h), indicated that PNEs might have the ability to cross the alveolar barrier.

3.7. Intracellular Uptake on H9c2 Cells

3.7.1. Time Dependence

The time dependence of endocytosis of Cou-6-B-PNE in H9c2 cells was illustrated in Fig. 5A-B. The intracellular Cou-6 increased within 8 h, at which time, the uptake of Cou-6-B-PNE plateaued, indicating the saturation of cellular uptake. according to this result, the time of pre-uptake was set at 2 h for subsequent drug effect experiment. Similarly, only a small amount of colocalization of lysosome and Cou-B-PNE was observed in the cytoplasm of H9c2 cells (Fig. 5C).

3.7.2. Drug Effect of P-PNE

Next, we used an emulsion with a therapeutic protein to evaluate for potential therapeutic effects. PEDF had been shown to play a central role in mediating cellular protection against oxidative stress, by promoting cell survival, reducing inflammation, and inhibiting pathological angiogenesis in a range of cell types and tissues. Our previous studies suggested that during oxygen-glucose deprivation (OGD), PEDF drove cardiomyocytes to low levels of ATP, and promoted glycogen accumulation to increase energy reserves, prolonged cell viability, and reduced cardiomyocyte apoptosis (Qiu et al., 2018) (Zhuang et al., 2016). We synthesized P-PNE loaded with PEDF to study whether the therapeutic nanoemulsion could protect cardiomyocytes. After pre-incubation of H9c2 cells with P-PNE for 2 h, compared with the OGD group, cleaved-caspase 3 and rip 3 expression was significantly decreased in embryonic rat heart cells treated with P-PNEs, demonstrating a reduction in cardiomyocyte death (Fig. 6A-B). This beneficial result suggests that formulation of PEDF with the phospholipid complex did not dramatically affect the activity of PEDF.

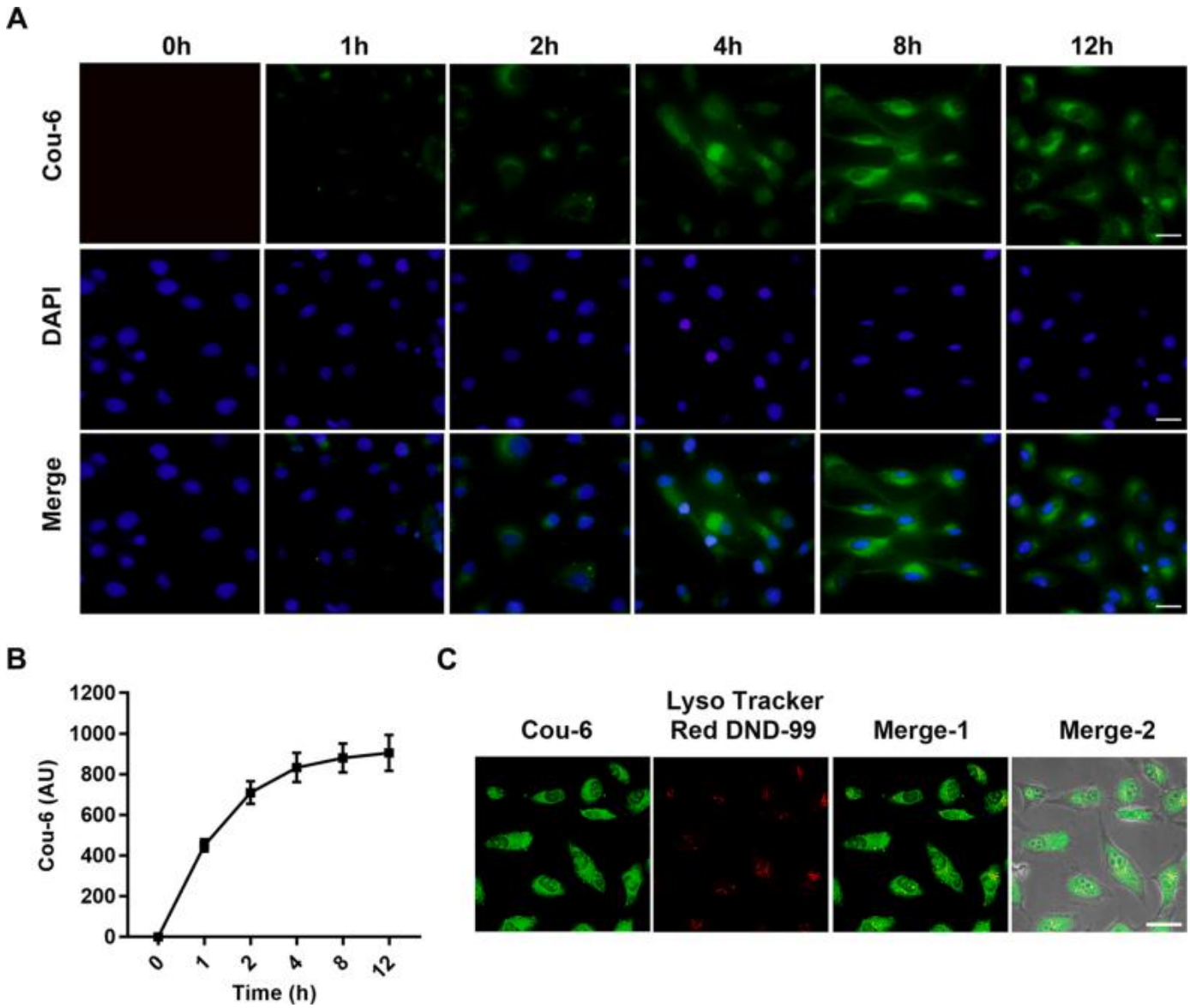

Fig. 5. PNEs are easily taken up by H9c2 cells. (A) Representative images (fluorescent microscopy) of the uptake time dependence of Cou-6-B-PNE. Coumarin 6 (green) in the cytoplasm; 40 × Objective lens; bar = 10 μm. (B) Quantitative measurement of the time dependence of intracellular uptake from using a multimode microplate reader (n=3). (C) The localization of Cou-6-B-PNE in the H9c2 cells. 60 × Objective lens; bar = 10 μm.

3.8. Biodistribution of Proteins in Rat Myocardial Tissue

In order to observe whether the PNEs were able to reach heart, we first labeled proteins with Cy5 to prepare Cy5-PNEs (Cy5-B-PNE and Cy5-P-PNE). The immunofluorescence observation results of lung tissue sections showed that PNEs were successfully delivered to the lungs and existed for up to 12h (Fig. 7). According to this result, we choose 6 hours as the time for observing the condition of myocardial tissue uptake. Six hours after treatment by inhalation, red scattered fluorescence was observed in myocardial tissue sections, indicating that the PNEs had successfully translocated from the respiratory tract to the heart and were taken up by myocardial tissue (Fig. 8A). Similarly, the western blot of rat myocardial tissue confirmed this result. Compared with the normal group, the relative signal of PEDF in the myocardial tissue of the P-PNE group increased 2-fold. Of note, the abundance of PEDF in myocardial tissues was not significantly increased in rats treated with PEDF in aqueous solution (Fig. 8B-C).

3.9. Inhalation of PNEs to Reduce Rat Myocardial Infarct Size and Promote Glycogen Accumulation

Finally, we evaluated the efficacy of PNEs with pharmacodynamic experiments *in vivo* . Previous studies have shown that lentiviral over-expression of PEDF increased glycogen accumulation and reduced the area of myocardial infarction in rats with acute myocardial infarction (Yuan et al., 2019). However, in contrast from previous studies, we delivered recombinant rat PEDF to the rat myocardium in the form of inhaled P-PNE in this work. Six hours after inhaling P-PNE, left anterior descending coronary artery was ligated to establish a rat model of AMI to evaluate the therapeutic effect of PEDF protein. Encouragingly, 6 h after AMI, TTC staining showed that the infarct area of the P-PNE--treated group was significantly smaller, representing that it effectively prevented myocardial damage caused by acute ischemia, however the group treated with aqueous PEDF was not protected (Fig. 9A-B). Glycogen staining also showed that the ischemic area of myocardial tissue from the P-PNE-treated group had higher glycogen accumulation compared to the control or PEDF group (Fig. 9C-D). These results

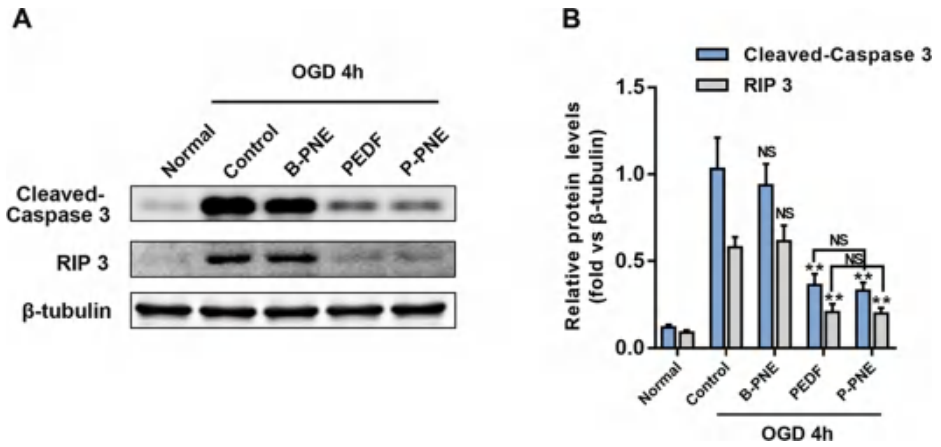

Fig. 6. P-PNE could exert the therapeutic effect of PEDF. (A) Western blot for cleaved caspase-3 and rip 3 in H9c2 cells subjected to OGD for 4 h after treatment with emulsions or equal volumes of solution for 2 h (proteins, 0.5 μg / ml). (B) Densitometric analysis of cleaved caspase-3 and rip 3 protein. Data are expressed as mean ± SD (n = 3). NS, **P < 0.01 vs Control group (OGD 4h). NS vs indicated group.

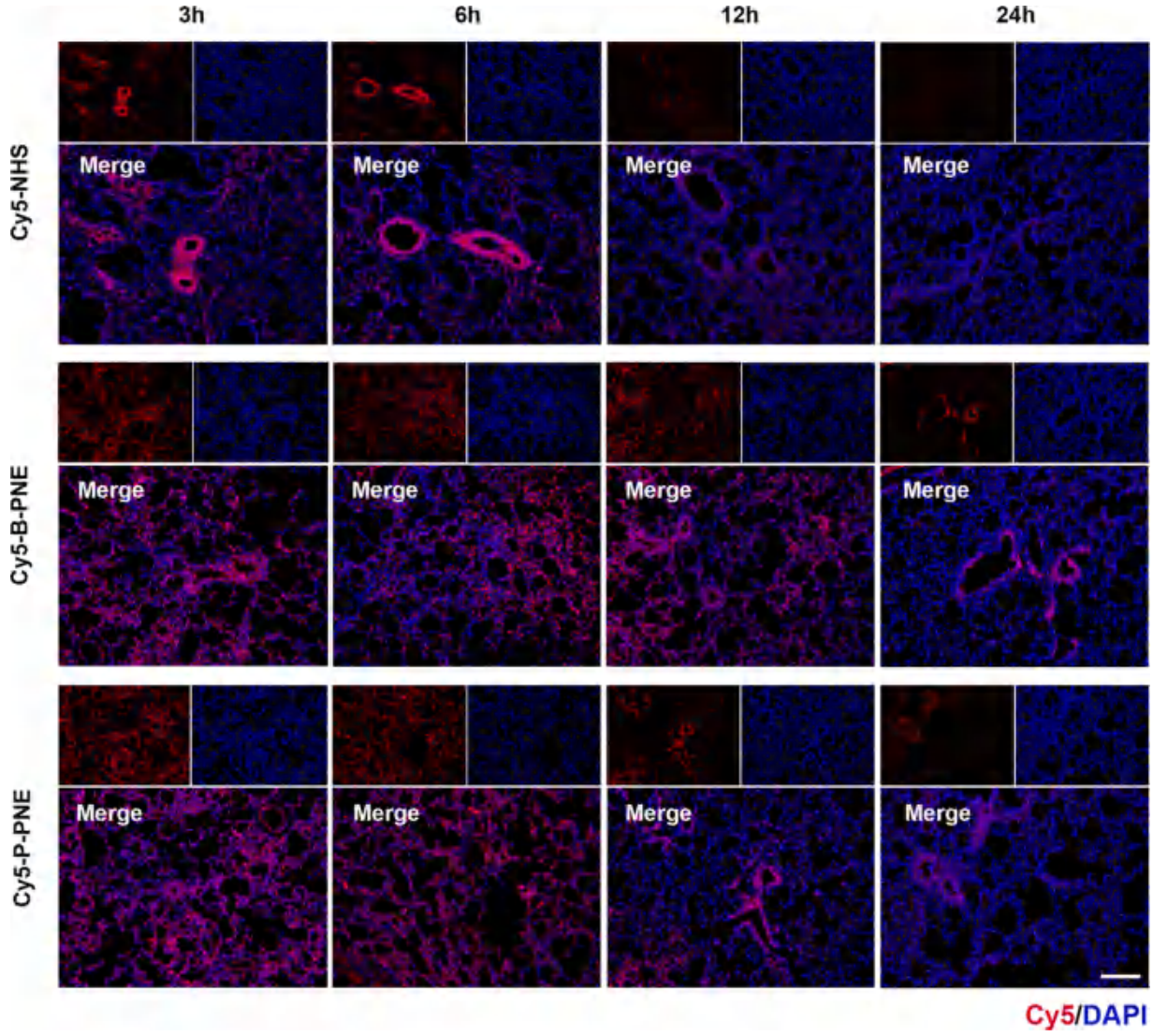

Fig. 7. Inhalation of PNEs. Immunofluorescence analysis of the expression and distribution of Cy5 in rat lung tissues, 3, 6, 12, 24 hours after inhaling Cy5-PNEs or equal volumes of Cy5-NHS solution. Cy5 (red); DAPI (blue); 10 × Objective lens; bar = 100 μm.

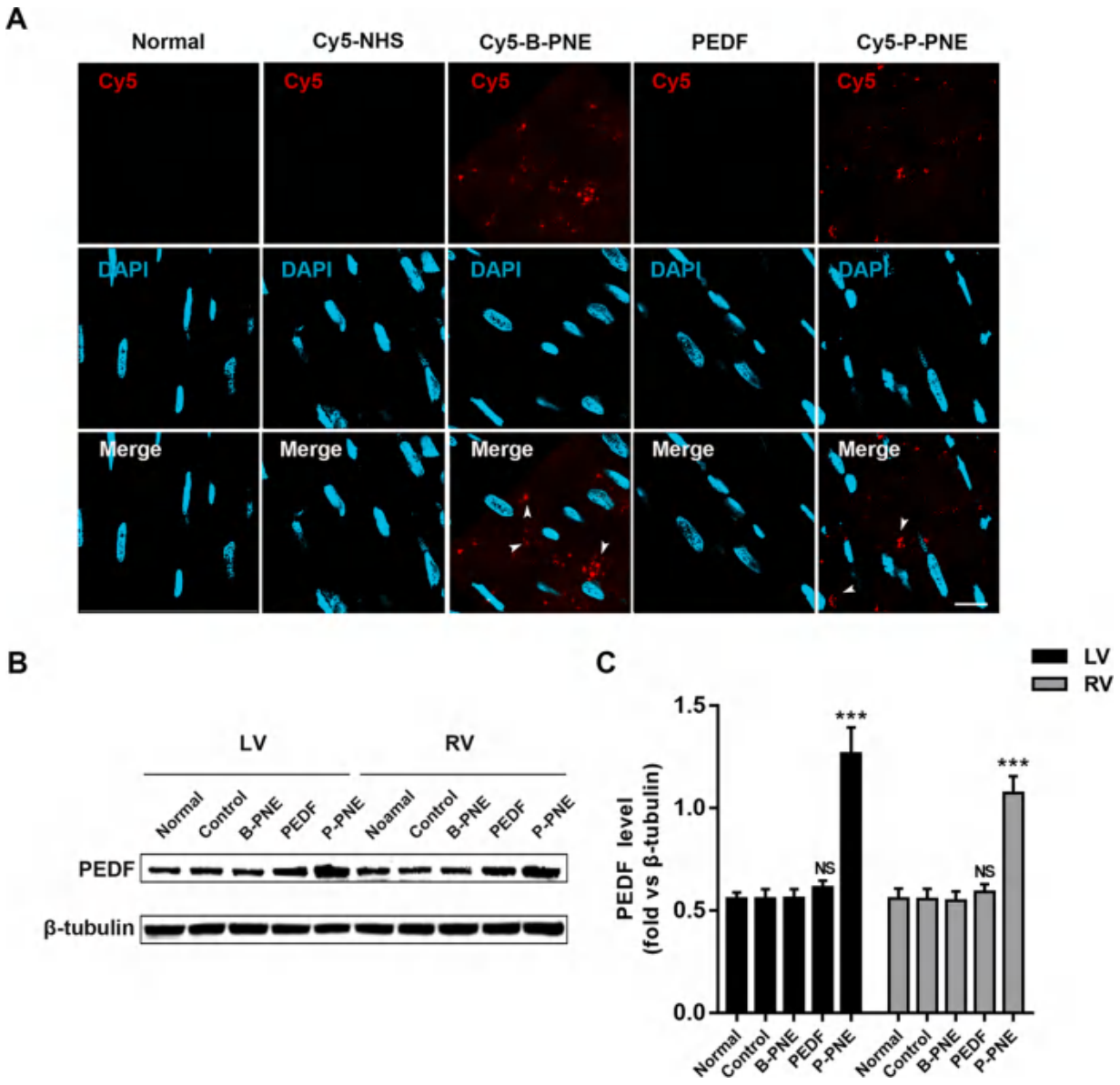

Fig. 8. Inhaled PNEs deliver proteins to rat myocardial tissue. (A) Confocal immunofluorescence analysis of the expression and distribution of Cy5 in rat myocardial tissues, eight hours after inhaling Cy5-P-PNE and Cy5-B-PNE or equal volumes of Cy5-NHS solution. The white arrow indicates the area of Cy5-PNEs. Cy5 (red); DAPI (blue); 60 × Objective lens; bar = 10 μm. (B) Western blot for PEDF in rat myocardial tissues, eight hours after inhaling emulsions or equal volumes of normal saline (proteins, 2 mg/kg). (C) Densitometric analysis of PEDF protein. Data are expressed as mean ± SD (n = 3). NS, ***P < 0.001 vs Control group (normal saline group). LV, left ventricle; RV, right ventricle.

suggested that PNE formulation helped to deliver the protein to the myocardium where it could exert therapeutic effects.

3.10. Inhalation of PNEs to Maintain Arterial Oxygen Partial Pressure

During inhalation, transient respiratory depression may occur. To observe the effects of application of PNEs, we collected arterial blood and treated rats with an inhaled dose of PNEs every two days for a total of 6 treatments to assess potential side effects. The result showed that, although PaO_2 in each group was within the normal physiological reference range (80-100 mmHg), PaO_2 value after inhalation of PNEs was significantly higher than the NS group (Fig. 10A), which might be related to the oxygen-carrying function of PFOB. In addition, no significant damage was observed in rat lung and heart tissues after a total of 6 treatments (Fig. 10B). TNF-α, IL-1β and IL-6 are generally considered as biomarkers of lung inflammation damage (Luo et al., 2020), analysis of them expression in the BALF does not reveal any significant changes in protein expression (Fig. 10C-E).

4. Discussion

In this study, an inhalable, protein-loaded PFC nanoemulsion was developed for the prevention and treatment of heart disease. Nanoemulsions have size distribution ranging between 50 and 1000 nm with a mean droplet size of about 250 nm (Tamilvanan, 2009). Small particle sizes and high bioavailability are highly desirable characteristics for respiratory formulations. With a particle size of ~140 nm, our PNEs perfectly fit within this size range (Fig. 2A-C). Although nanoemulsions have been used for many forms of drug delivery, most respiratory research has focused on formulations of small molecule drugs, and most research on protein-loaded nanoemulsions has focused on oral administration (Rajpoot et al., 2011). We combined the properties of protein-phospholipid complexes and PFC emulsions to synthesize PNEs, with the goal of delivering protein to the heart. Our findings suggested

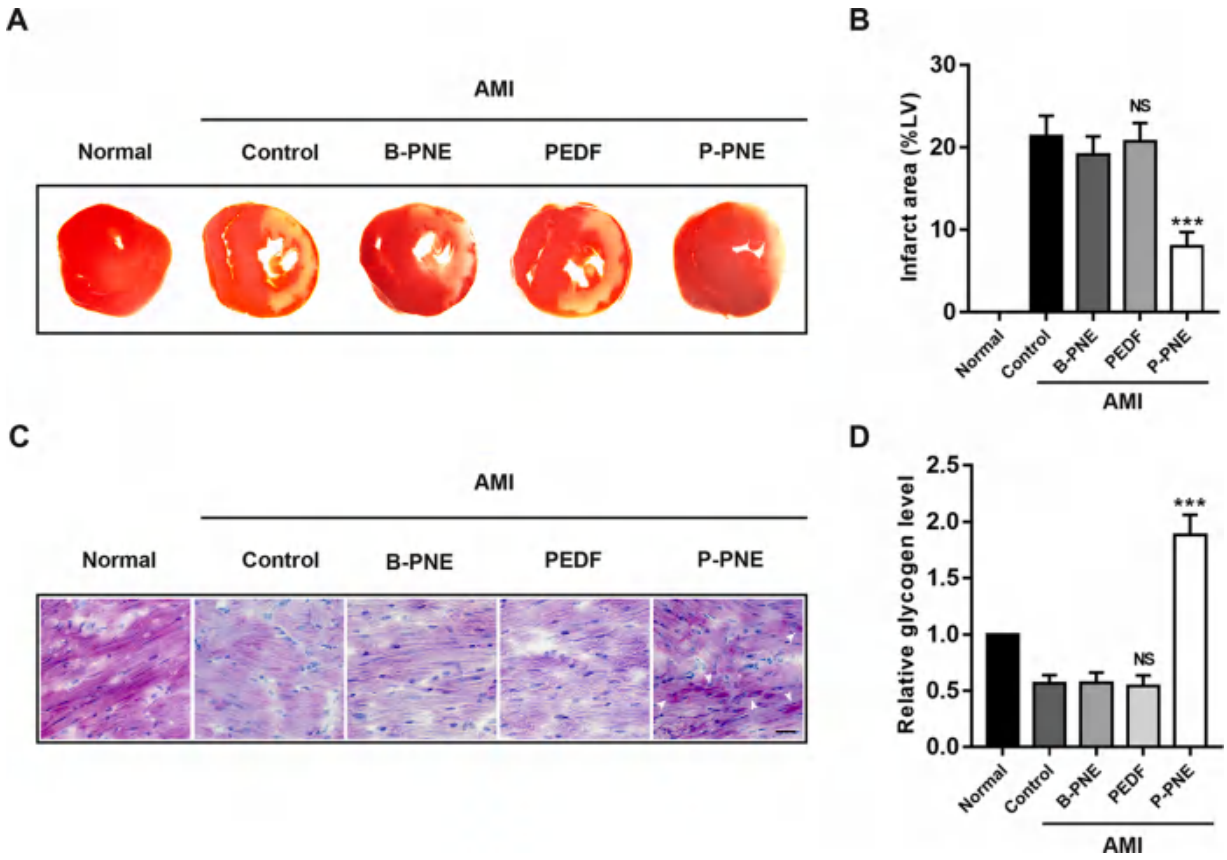

Fig. 9. Inhaled P-PNE reduce myocardial infarct size and increase glycogen deposition in ischemic areas. (A) Representative images of the TTC staining of myocardial tissues after AMI. Pale areas indicate infarcted regions. (B) Quantification of myocardial infarct size (INF) expressed as a percentage of the left ventricle (LV). (B) PAS staining images of myocardial ischemic areas, as observed by light microscopy. The white arrow indicates the area of glycogen. 40 × Objective lens; bar = 20 μm. (C) Quantification of glycogen content. Data are expressed as mean ± SD. NS, ***P < 0.001 vs Control group (AMI) (n = 6, each group).

that this is a feasible strategy: PNEs delivered therapeutic proteins to the myocardial tissue from respiratory tract, and exerted a protective effect against ischemia.

PFCs are biocompatible materials that have been studied for a range of biomedical applications, for example, PFOB has been used as a respiratory medium in animals and humans during liquid ventilation (Kohlhauer et al., 2016). PFCs display weak intermolecular interactions and are highly volatile, which can be quickly cleared from the lung or systemic circulation by exhalation (Lehmler, 2007). PFCs can be taken up by many types of cells by phagocytosis (Flaim, 1994). Extracellular uptake experiments confirm that PNEs are easily taken up by cardiomyocytes (Fig. 5A). Interestingly, we find that PNEs make proteinaceous drugs show a wider distribution in the lungs (Fig. 7). In addition, our study provides a possibility to enhance stability of proteinaceous drugs as PFCs can protect proteins from lysosomal degradation (Fig. 4). Finally, we also check the possible side effects of long-term inhalation of PNEs. Certain cytokines and biomarkers have been studied well for the role in inflammation. TNF-α, IL-1β and IL-6 are pro-inflammatory cytokines that are responsible for the enhanced production of other cytokines and augmentation of damage (Bagaria et al., 2020). We find that PNEs do not cause an increase in cytokine expression (Fig. 10C-E). Supporting this result, there are no observable pathologies in the heart or lung slices (Fig. 10B). This suggests that intrapulmonary delivery of drug emulsion does not cause inflammation.

Compared with intravenous injection, inhalation delivery will always provide slightly slower absorption. However, the treatment of cardiovascular diseases is usually chronic and long-term. Importantly, pulmonary delivery does not require professional injection in a clinical setting. Further, it is more accepted by patients. In addition, the use of a PFC-based nanoemulsion may help to avoid respiratory depression caused by inhalation. This may provide significant benefits for elderly patients with underlying lung disease. However, this study had several important limitations. Under normal physiological conditions, increases in specific surface proteins (such as cardiac troponin) usually occur after AMI rather than before (Kimenai et al., 2016), so it is difficult for PNEs to exert targeted effects. In addition, we did not study the pharmacokinetics of PNEs. Further research is needed to answer these remaining questions.

5. Conclusion

In this study, protein-loaded PFC nanoemulsions with a diameter of about 140 nm were prepared by a simple extrusion method and used as an inhaled treatment to reduce the effects of AMI in a rat model of disease. The cytotoxicity of PNEs was assessed by cell viability assays and measurement of apoptotic cells. In addition, the fine particle fraction and protein release kinetics supported the feasibility of inhalation of aerosolized PNEs. Translocation studies indicated that PNEs had the potential to cross the pulmonary alveolar epithelial barrier. Compared to aqueous proteins, PNE-formulation led to greater uptake in rat myocardial tissues, as demonstrated by immunofluorescence and western blotting analysis. Measurements of infarct size and glycogen deposition demonstrated that treatment with the emulsion had significant therapeutic effects. These results support this formulation method as a delivery platform suitable for a broad range of therapeutic proteinaceous drugs and opens a new direction for the treatment of cardiovascular diseases.

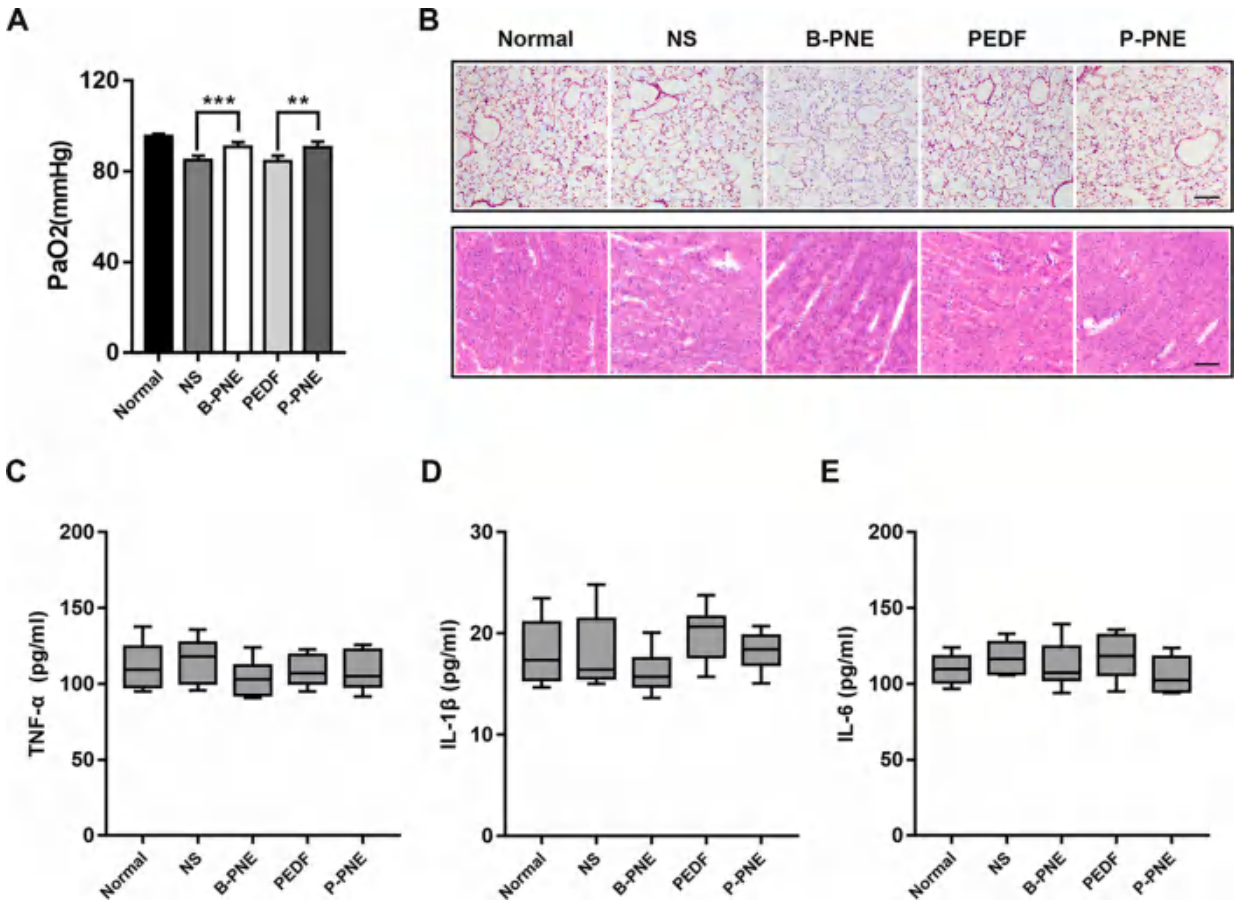

Fig. 10. Blood gas analysis and pathology images of rats. (A) PaO_2 of rats that inhaled PNEs or an equivalent volume normal saline. Data are expressed as mean ± SD (n = 6). ***P < 0.001, **P < 0.01 vs indicated group. (B) Lung sections (H&E). All biopsy sections were taken from the rats sacrificed after a total of 6 treatments; 20 × Objective lens; bar = 100 μm. H&E, hematoxylin and eosin. (C), (D) and (E) Quantification of cytokines. Compared with the normal group, the expression of TNF-α, IL-1β and IL-6 did not change significantly (p <0.05).

Declaration of Competing Interest

The authors declare that they have no conflict of interest.

Acknowledgements

This work was supported by the grant from National Nature Science Foundation of China (81570242 and 81502995), the Social Development Projects of Key R&D Programs in Jiangsu Province (BE2019643), the Science and Technology Project of (KC19068), the key R&D Plan (Social Development) of Xuzhou city (KC18206) and the Postgraduate Research&Practice Innovation Program of Jiangsu Province (KYCX20_2498).

References

Bull, SC, Doig, AJ., 2015. Properties of protein drug target classes. PloS one 10 (3), e0117955. https://doi.org/10.1371/journal.pone.0117955.

Lagasse, HA, Alexaki, A, Simhadri, VL, et al., 2017. Recent advances in (therapeutic protein) drug development. F1000Research 6, 113. https://doi.org/10.12688/f1000research.9970.1.

Prince, MJ, Wu, F, Guo, Y, et al., 2015. The burden of disease in older people and implications for health policy and practice. Lancet 385 (9967), 549–562. https://doi.org/10.1016/S0140-6736(14)61347-7.

Liu, M, Li, M, Wang, G, et al., 2014. Heart-targeted nanoscale drug delivery systems. Journal of biomedical nanotechnology 10 (9), 2038–2062. https://doi.org/10.1166/jbn.2014.1894.

Puisney, C, Baeza-Squiban, A, Boland, S., 2018. Mechanisms of Uptake and Translocation of Nanomaterials in the Lung. Adv Exp Med Biol 1048, 21–36. https://doi.org/10.1007/978-3-319-72041-8_2 [published Online First: 2018/02/18].

Miragoli, M, Ceriotti, P, Iafisco, M, et al., 2018. Inhalation of peptide-loaded nanoparticles improves heart failure. Science translational medicine 10 (424). https://doi.org/10.1126/scitranslmed.aan6205.

Asmawi, AA, Salim, N, Ngan, CL, et al., 2019. Excipient selection and aerodynamic characterization of nebulized lipid-based nanoemulsion loaded with docetaxel for lung cancer treatment. Drug Deliv Transl Res 9 (2), 543–554. https://doi.org/10.1007/s13346-018-0526-4 [published Online First: 2018/04/25].

Arbain, NH, Salim, N, Masoumi, HRF, et al., 2019. In vitro evaluation of the inhalable quercetin loaded nanoemulsion for pulmonary delivery. Drug Deliv Transl Res 9 (2), 497–507. https://doi.org/10.1007/s13346-018-0509-5 [published Online First: 2018/03/16].

Jaafar-Maalej, C, Andrieu, V, Elaissari, A, et al., 2009. Assessment methods of inhaled aerosols: technical aspects and applications. Expert opinion on drug delivery 6 (9), 941–959. https://doi.org/10.1517/17425240903117244.

Braakhuis, HM, Kloet, SK, Kezic, S, et al., 2015. Progress and future of in vitro models to study translocation of nanoparticles. Arch Toxicol 89 (9), 1469–1495. https://doi.org/10.1007/s00204-015-1518-5 [published Online First: 2015/05/16].

Naahidi, S, Jafari, M, Edalat, F, et al., 2013. Biocompatibility of engineered nanoparticles for drug delivery. Journal of controlled release: official journal of the Controlled Release Society 166 (2), 182–194. https://doi.org/10.1016/j.jconrel.2012.12.013.

Braakhuis, HM, Gosens, I, Krystek, P, et al., 2014. Particle size dependent deposition and pulmonary inflammation after short-term inhalation of silver nanoparticles. Part Fibre Toxicol 11, 49. https://doi.org/10.1186/s12989-014-0049-1 [published Online First: 2014/09/18].

Li, X, Sui, Z, Li, X, et al., 2018. Perfluorooctylbromide nanoparticles for ultrasound imaging and drug delivery. International journal of nanomedicine 13, 3053–3067. https://doi.org/10.2147/IJN.S164905.

Lehmler, HJ., 2007. Perfluorocarbon compounds as vehicles for pulmonary drug delivery. Expert opinion on drug delivery 4 (3), 247–262. https://doi.org/10.1517/17425247.4.3.247.

Lowe, KC., 1999. Perfluorinated blood substitutes and artificial oxygen carriers. Blood reviews 13 (3), 171–184. https://doi.org/10.1054/blre.1999.0113.

Tombran-Tink, J, Barnstable, CJ., 2003. PEDF: a multifaceted neurotrophic factor. Nature reviews Neuroscience 4 (8), 628–636. https://doi.org/10.1038/nrn1176.

Brook, N, Brook, E, Dharmarajan, A, et al., 2020. Pigment epithelium-derived factor regulation of neuronal and stem cell fate. Experimental cell research, 111891. https://doi.org/10.1016/j.yexcr.2020.111891.

Yuan, Y, Liu, X, Miao, H, et al., 2019. PEDF increases GLUT4-mediated glucose uptake in rat ischemic myocardium via PI3K/AKT pathway in a PEDFR-dependent manner. International journal of cardiology 283, 136–143. https://doi.org/10.1016/j.ijcard.2019.02.035.

Qiu, F, Zhang, H, Yuan, Y, et al., 2018. A decrease of ATP production steered by PEDF in cardiomyocytes with oxygen-glucose deprivation is associated with an AMPK-dependent degradation pathway. International journal of cardiology 257, 262–271. https://doi.org/10.1016/j.ijcard.2018.01.034.

Rao, SV, Shao, J., 2008. Self-nanoemulsifying drug delivery systems (SNEDDS) for oral delivery of protein drugs: I. Formulation development. International journal of pharmaceutics 362 (1-2), 2–9. https://doi.org/10.1016/j.ijpharm.2008.05.018.

Zhang, Q, He, N, Zhang, L, et al., 2012. The in vitro and in vivo study on self-nanoemulsifying drug delivery system (SNEDDS) based on insulin-phospholipid complex. Journal of biomedical nanotechnology 8 (1), 90–97. https://doi.org/10.1166/jbn.2012.1371.

Tencer, M, Charbonneau, R, Lahoud, N, et al., 2007. AFM study of BSA adlayers on Au stripes. Applied Surface Science 253 (23), 9209–9214. https://doi.org/10.1016/j.apsusc.2007.05.079.

Becerra, SP., 2006. Focus on Molecules: Pigment epithelium-derived factor (PEDF). Exp Eye Res 82 (5), 739–740. https://doi.org/10.1016/j.exer.2005.10.016 [published Online First: 2005/12/21].

Khan, J, Alexander, A, Ajazuddin, et al., 2013. Recent advances and future prospects of phyto-phospholipid complexation technique for improving pharmacokinetic profile of plant actives. Journal of controlled release: official journal of the Controlled Release Society 168 (1), 50–60. https://doi.org/10.1016/j.jconrel.2013.02.025 [published Online First: 2013/03/12].

Jiang, LQ, Wang, TY, Wang, Y, et al., 2019. Co-disposition of chitosan nanoparticles by multi types of hepatic cells and their subsequent biological elimination: the mechanism and kinetic studies at the cellular and animal levels. International journal of nanomedicine 14, 6035–6060. https://doi.org/10.2147/IJN.S208496 [published Online First: 2019/09/20].

Li, J, Peng, C, Guo, Z, et al., 2018. Radioiodinated Pentixather for SPECT Imaging of Expression of the Chemokine Receptor CXCR4 in Rat Myocardial-Infarction-Reperfusion Models. Analytical chemistry 90 (15), 9614–9620. https://doi.org/10.1021/acs.analchem.8b02553.

Zhou, C, Xia, X, Liu, Y, et al., 2012. The preparation of a complex of insulin-phospholipids and their interaction mechanism. Journal of peptide science: an official publication of the European Peptide Society 18 (9), 541–548. https://doi.org/10.1002/psc.2423.

Yuan, Y, Huang, B, Miao, H, et al., 2019. A "Hibernating-Like" Viable State Induced by Lentiviral Vector-Mediated Pigment Epithelium-Derived Factor Overexpression in Rat Acute Ischemic Myocardium. Human gene therapy 30 (6), 762–776. https://doi.org/10.1089/hum.2018.186.

Liu, Y, Zhang, P, Feng, N, et al., 2009. Optimization and in situ intestinal absorption of self-microemulsifying drug delivery system of oridonin. International journal of pharmaceutics 365 (1-2), 136–142. https://doi.org/10.1016/j.ijpharm.2008.08.009.

Gonzalez-Rothi, RJ, Straub, L, Cacace, JL, et al., 1991. Liposomes and pulmonary alveolar macrophages: functional and morphologic interactions. Experimental lung research 17 (4), 687–705. https://doi.org/10.3109/01902149109062873.

Courrier, HM, Krafft, MP, Butz, N, et al., 2003. Evaluation of cytotoxicity of new semi-fluorinated amphiphiles derived from dimorpholinophosphate. Biomaterials 24 (4), 689–696. https://doi.org/10.1016/s0142-9612(02)00407-6.

Shi, Q, Huang, Y, Chen, X, et al., 2009. Hemoglobin conjugated micelles based on triblock biodegradable polymers as artificial oxygen carriers. Biomaterials 30 (28), 5077–5085. https://doi.org/10.1016/j.biomaterials.2009.05.082.

Zhuang, W, Zhang, H, Pan, J, et al., 2016. PEDF and PEDF-derived peptide 44mer inhibit oxygen-glucose deprivation-induced oxidative stress through upregulating PPARgamma via PEDF-R in H9c2 cells. Biochemical and biophysical research communications 472 (3), 482–488. https://doi.org/10.1016/j.bbrc.2016.02.110.

Luo, Y, Pang, XX, Ansari, AR, et al., 2020. Visfatin Exerts Immunotherapeutic Effects in Lipopolysaccharide-Induced Acute Lung Injury in Murine Model. Inflammation 43 (1), 109–122. https://doi.org/10.1007/s10753-019-01100-3 [published Online First: 2019/11/07].

Tamilvanan, S., 2009. Formulation of multifunctional oil-in-water nanosized emulsions for active and passive targeting of drugs to otherwise inaccessible internal organs of the human body. International journal of pharmaceutics 381 (1), 62–76. https://doi.org/10.1016/j.ijpharm.2009.08.001.

Rajpoot, P, Pathak, K, Bali, V., 2011. Therapeutic applications of nanoemulsion based drug delivery systems: a review of patents in last two decades. Recent patents on drug delivery & formulation 5 (2), 163–172. https://doi.org/10.2174/187221111795471427.

Kohlhauer, M, Berdeaux, A, Kerber, RE, et al., 2016. Liquid Ventilation for the Induction of Ultrafast Hypothermia in Resuscitation Sciences: A Review. Ther Hypothermia Temp Manag 6 (2), 63–70. https://doi.org/10.1089/ther.2015.0024 [published Online First: 2016/02/26].

Flaim, SF., 1994. Pharmacokinetics and side effects of perfluorocarbon-based blood substitutes. Artif Cells Blood Substit Immobil Biotechnol 22 (4), 1043–1054. https://doi.org/10.3109/10731199409138801 [published Online First: 1994/01/01].

Bagaria, V, Mathur, P, Madan, K, et al., 2020. Predicting Outcomes After Blunt Chest Trauma-Utility of Thoracic Trauma Severity Score, Cytokines (IL-1beta, IL-6, IL-8, IL-10, and TNF-alpha), and Biomarkers (vWF and CC-16). Indian J Surg 1–7. https://doi.org/10.1007/s12262-020-02407-4 [published Online First: 2020/08/25].

Kimenai DM, Henry RM, van der Kallen CJ, et al. Direct comparison of clinical decision limits for cardiac troponin T and I. *Heart*2016;102(8):610-6.doi:10.1136/heartjnl-2015-308917.